Depth profile of spin and orbital magnetic moments in a subnanometer Pt film on Co

Motohiro Suzuki,[1,*] Hiroaki Muraoka,[2] Yuuki Inaba,[2] Hayato Miyagawa,[1] Naomi Kawamura,[1] Takehito Shimatsu,[2] Hiroshi Maruyama,[3] Naoki Ishimatsu,[3] Yoichi Isohama,[3] and Yoshiaki Sonobe[4]

[1]*SPring-8/JASRI, 1-1-1 Kouto, Mikazuki, Sayo, Hyogo 679-5198, Japan*

[2]*RIEC, Tohoku University, 2-1-1 Katahira, Sendai, Miyagi 980-8577, Japan*

[3]*Graduate School of Science, Hiroshima University, 1-3-1 Kagamiyama, Higashi-Hiroshima, Hiroshima 739-8526, Japan*

[4]*HOYA Corporation, 3280 Nakamaru, Nagasaka, Kitakoma, Yamanashi 408-8550, Japan*

(Received 26 September 2004; revised manuscript received 18 May 2005; published 19 August 2005)

The magnetic properties of a few atomic Pt layers on a 15-nm-thick Co film were studied by x-ray magnetic circular dichroism spectroscopy at the Pt $L_{2,3}$ edges. The spin and orbital magnetic moments of the Pt $5d$ electrons were separated using the sum rules, and the depth profiles of these moments were determined as a function of the distance from the Co-Pt interface. A Pt atom has a total magnetic moment of 0.61 μ_B/atom at the interface, and the moment decreases exponentially with the distance from the interface with a characteristic decay length of 0.41 nm. Four atomic Pt layers near the interface possess 90% of the total magnetization of Pt. The Pt orbital magnetic moment is more than 15% relative to the spin moment and confined to two atomic layers near the interface. The orbital moment was found to be isotropic in the dichroism measurements using external magnetic fields perpendicular and parallel to the film plane. These properties of Pt magnetization are discussed in the context of thermal stability of magnetic recording media covered with a thin Pt overlayer.

DOI: 10.1103/PhysRevB.72.054430 PACS number(s): 75.70.Cn, 78.70.Dm, 75.50.Ss

I. INTRODUCTION

The areal density of magnetic storage has steadily increased over the past decade. A recording density of 150 Gbits/in^2 was recently demonstrated in the laboratory,[1] and the bit dimension corresponds to 65×65 nm^2 in this medium. In order to achieve a higher density using perpendicular recording that employs smaller bit dimensions, the magnetic grain size of the recording medium should be correspondingly reduced to keep the number of grains within one bit cell constant and to keep the media noise within acceptable limits. In this context, another important feature of the high-density media is the thermal stability or the thermal demagnetization properties, which determine the long-time reliability of magnetic recording. The stability of a magnetic grain of volume V and anisotropy constant K_u can be approximated by K_uV/k_BT, where k_B is the Boltzmann constant and T is the temperature.[2,3] A magnetic grain is thermally stable if $K_uV/k_BT\gtrsim60$.[3] Thus, higher K_u materials have to be used in order to maintain the thermal stability in a high-density media with a smaller grain size. The increasing magnetic anisotropy of the material is vital for developing higher density recording media in the future.

Pt is a key material for high (perpendicular) magnetic anisotropy and for increasing the thermal stability in some layered magnetic materials. For instance, Co/Pt multilayer films[4] show a high perpendicular anisotropy with $K_u=8\times10^6$ erg/cm^3, which ensures the thermal stability of recording bits. In granular $CoCr_{18}Pt_{12}$ perpendicular media, a 1-nm Pt cap layer improves the thermal stability.[5] The Pt cap layer possibly has induced ferromagnetism, which gives rise to the large perpendicular anisotropy and increases the in-plane exchange coupling. As reported in Co/Pt multilayer systems[6–8] and Co-Pt alloys,[9–11] Pt atoms are significantly polarized in the vicinity of a ferromagnetic atom and can modify the magnetic properties of the entire system although elemental Pt is paramagnetic.

In this paper, we investigated the magnetic properties of single Pt layers that are less than 2-nm thick and located on a Co film, using x-ray magnetic circular dichroism (XMCD) spectroscopy at the Pt $L_{2,3}$ edges. The purpose of this study is to determine the fundamental magnetic nature of the Pt atoms adjacent to a magnetic layer like Co, which is generally applied in layered magnetic materials of strong magnetic anisotropy or high thermal stability. Several Pt/Co bilayer films were investigated as models for real recording media that have Pt layers between or on top of the magnetic layers. In particular, we have targeted layered films composed of a relatively thick ($\approx$15 nm) ferromagnetic layer and a thin nonmagnetic Pt overlayer, such as those treated in Ref. 5. We use the element specificity of the XMCD technique to probe the magnetization of only a few atomic Pt layers. The spin and orbital magnetic moments of the Pt $5d$ electrons were separated and the anisotropy of the orbital and magnetic dipole moments was addressed. The depth profile of these moments as a function of the distance from the Co-Pt interface were determined from a series of the XMCD data obtained using samples of varying Pt layer thicknesses.

II. EXPERIMENT

A. Pt/Co bilayer films

The Pt/Co bilayer films were prepared by dc magnetron sputtering at room temperature. A magnetic Co layer, approximately 15-nm thick, was deposited on a glass substrate; subsequently, a Pt layer was deposited on top. Before the Co deposition, a 10-nm Ti underlayer was deposited on the glass to create a texture for the magnetic film. Samples with four different Pt thicknesses $t=0.15$, 0.5, 1, and 2 nm were prepared by regulating the sputter growth time after careful calibration of the Pt deposition rate.

TABLE I. Characteristics of Pt/Co bilayer films. t and t_{Co} denote the thicknesses of the Pt and Co layer, respectively. σ denotes the roughness of the Co-Pt interface and $\Delta\theta_{50}$ denotes the angular dispersion of the Co c axis.

t(nm)	t_{Co}(nm)	σ(nm)	$\Delta\theta_{50}$(°)
0.15	14.0	0.9	13.4
0.5	14.3	1.0	9.5
1.0	14.8	1.1	10.8
2.0	14.6	1.1	9.0

Characteristics of the samples are summarized in Table I. The Pt thicknesses listed in the table are designed values, which are consistent with the relative intensities of x-ray absorption spectra (XAS) determined in a separate measurement. The Co thickness t_{Co} and Co-Pt interface roughness σ were determined by low-angle x-ray reflectometry. Analysis of the reflectivity data using the designed value of Pt thickness yielded a good fitting result. Since assuming an alloying layer between Pt and Co layers did not improve the fitting accuracy of the reflectivity profile, the possibility of significant interface alloying is excluded.[12] The interface roughness is approximately 1 nm and nearly constant for all films. This is possibly a result from the lateral long-range and constant roughness of the substrate or the Ti underlayer. Thus, it is not surprising that the interface roughness values are larger than the Pt layer thickness in the small coverage films. The lateral short-range roughness of the Co-Pt interface could be much smaller.

Figure 1 shows x-ray diffraction profiles measured using Cu K_α radiation. Overlapping diffraction peaks of Co hcp (0002) and Co fcc (111) were observed. Diffraction intensities from other lattice planes were not observed. This result indicates that the closed-packed plane of the Co layer was grown parallel to the film plane. The normal to the closed-packed plane is oriented perpendicular to the film plane with an angular distribution of typically 10°, given by $\Delta\theta_{50}$, the full width half maxima of the x-ray rocking curve (not shown). The Pt diffraction peak was observed at the low angle side of the Co peak only for the t=2-nm sample. The appearance of a broad peak for the largest coverage, around

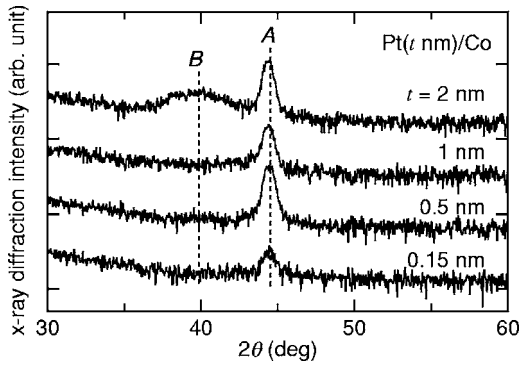

FIG. 1. X-ray diffraction profiles of Pt(t nm)/Co bilayer films for t=0.15, 0.5, 1, and 2 nm. The vertical lines indicate the 2θ value corresponding to the A:hcp Co (0002) and B:fcc Pt (111) reflections.

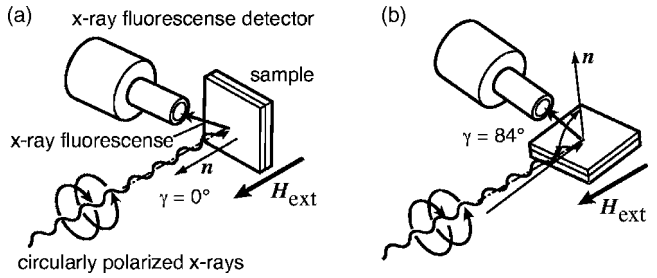

FIG. 2. Setup scheme for x-ray magnetic circular dichroism measurement in (a) normal (γ=0°) and (b) grazing (γ=84°) incidence of x rays.

the position of bulk fcc Pt, shows that the Pt layer was grown with grains of a partial (111) texture. However, no clear diffraction pattern was obtained from samples with a thinner Pt layer because the thickness is not sufficient to form a diffraction pattern.

Magnetic properties were characterized by standard vibrating sample and torque magnetometry at room temperature. Measured magnetization (M vs. H) curves showed that an easy magnetization axis exists within the film plane. The in-plane saturation magnetization M_s=1350±100 emu/cm^3 is identical for all films within the experimental error. The magnetocrystalline anisotropy constant of the Co layer is $K_1+K_2=4.0\times10^6$ erg/cm^3, which is smaller than the value reported for a single crystalline hcp Co(0001) film (5.7×10^6 erg/cm^3).[13] The reduced anisotropy in our polycrystalline film is probably due to stacking faults or the presence of fcc Co formed primarily near the interface of the Ti underlayer. All the present samples do not exhibit perpendicular magnetic anisotropy because the K_1+K_2 is one third of the demagnetizing field energy $2\pi M_s^2$.

B. XMCD experiments

The XMCD experiments were performed at BL39XU of SPring-8 synchrotron radiation facility.[14] Helicity-switchable circularly polarized x rays of a high degree of circular polarization ($\geqslant$95%) were available by using a diamond x-ray phase retarder. Figure 2 shows the experimental arrangement with (a) normal and (b) grazing incidence of x rays on the sample. Spectra of a Pt/Co film were recorded in an external magnetic field parallel to the x-ray propagation direction, at angles γ=0° and 84° with respect to the surface normal. In both arrangements, the sample magnetization was saturated by a 20 kOe magnetic field generated by an electromagnet.

For each configuration, the helicity-dependent x-ray absorption spectrum was determined by monitoring the x-ray fluorescence yield from the sample by reversing the photon helicity at 0.5 Hz while the x-ray energy E was scanned around the Pt L_3 and L_2 edges, with the direction of magnetization maintained constant. In this manner, two helicity-dependent spectra $I^+(E)$ and $I^-(E)$, where $I^+(E)[I^-(E)]$ denotes the intensity when the incident photon momentum and the magnetization vectors are parallel [antiparallel], were recorded simultaneously. The XMCD spectrum is given by the difference of the two spectra

$$\Delta I(E) = I^{-}(E) - I^{+}(E) \quad (1)$$

and the polarization-averaged XAS spectrum is defined by

$$I(E) = [I^{-}(E) + I^{+}(E)]/2. \quad (2)$$

Instrumental asymmetries were verified by reacquiring the XMCD spectra for the reversed magnetization direction.

X-ray fluorescence yields were measured using a silicon drift detector (RÖNTEC, XFlash® Detector 1000),[15] which is operational with a total photon count as high as 10^5 counts/s and has a moderate energy resolution of $\approx$300 eV. In our experiments, we estimated the total dead time of the detector system, including that of the detector and the associated electronics, to be 1.1 μs. The measured output counts of the detector were corrected using a nonparalyzable model. This correction was responsible for the resulting linearity of the detector response better than 0.5% at a total photon input rate of up to 2×10^5 counts/s despite a 15% counting loss without correction. These detector performances allowed for efficient separation of the Pt L_α (L_3 excitation) and the L_β (L_2 excitation) lines from the intense elastic scattering from the thick substrate and fluorescence lines from the Co layer. Consequently, weak fluorescence signals from a Pt layer of thinner than 2 nm were detected with a sufficiently high sensitivity despite excitation by hard x rays with a large penetration depth of more than a few microns.

III. RESULTS AND DISCUSSION

A. XMCD spectra

Figure 3(a) shows the XMCD spectra of Pt/Co films with various Pt thickness, measured at the Pt L_3 ($2p_{3/2}\rightarrow5d$ valence) and Pt L_2 ($2p_{1/2}\rightarrow5d$ valence) edges. Polarization-averaged XAS spectra are compared in Fig. 3(b). These spectra were obtained for the $\gamma=0^\circ$ configuration. The XMCD and XAS spectra include the same scale factor such that the XAS step height is 2.07 at the L_3 edge and 1.00 at the L_2 edge. This branching ratio was experimentally determined from the XAS measurement of the present samples. In determining the ratio, we applied strict corrections to the sensitivity of the incident x-ray intensity monitor, dead time of the fluorescence detector, and attenuation of the air path and attenuators in front of the detector.

The spectra exhibit a clear dichroism effect. The sign of the XMCD spectra was negative at the L_3 edge and positive at the L_2 edge, indicating that the magnetization of the Pt layer is parallel to the external field and to the magnetization of the Co layer. At both the L_3 and L_2 edges, the dichroism effect weakened with increasing Pt thickness, indicating that the Pt magnetization is concentrated near the Co-Pt interface and decreases with the increase in distance from the interface. The shape of the XMCD spectra does not depend on the Pt thickness. The feature of the XAS spectra changes with the Pt thickness; this is discussed in Sec. III B in the context of the interface character.

The 0.15-nm-thick Pt sample exhibits the largest XMCD effect, 22% relative to the XAS edge step height. This value is, to the best of our knowledge, larger than any XMCD data of Pt in Pt-transition metal alloys[9–11] Co/Pt (Ref. 6) and Ni/Pt multilayers,[16] reported to date. Since most Pt atoms in the 0.15-nm sample are adjacent to the Co layer, the Pt atoms located very close to the Co-Pt interface may have a considerable magnetic moment.

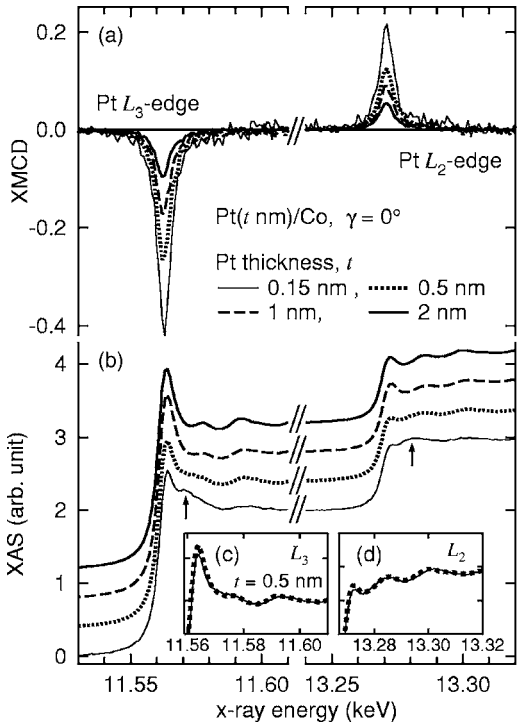

FIG. 3. (a) X-ray magnetic circular dichroism (XMCD) and (b) x-ray absorption spectra (XAS) of Pt(t nm)/Co bilayers, measured at the Pt $L_{2,3}$ edges at $\gamma=0°$. The measured (line) and generated (dots) XAS spectra of the $t=0.5$-nm sample are compared at the (c) L_3 and (d) L_2 edges.

Figure 4 compares the XMCD spectra measured at $\gamma=0^\circ$ and 84°. The variations with the Pt layer thickness in both configurations were in good agreement; XMCD amplitude decreases with increasing the Pt thickness. The dependence of the amplitude on the direction of magnetization is observed in thin Pt samples for $t=0.15$ and 0.5 nm; XMCD amplitude at $\gamma=0^\circ$ is larger than that at $\gamma=84^\circ$. In the case of thick Pt samples, $t=1$ and 2 nm, the XMCD amplitudes are independent of the direction of magnetization. This result suggests that a certain magnetic anisotropy exists near the Co-Pt interface, and the anisotropy may be negligible at a distance of more than 1 nm from the interface.

B. XAS spectra and interface character

In this subsection, we use the XAS structure varying with Pt thickness to discuss the electronic states of the Pt cap layer with reference to the interface character. In Fig. 3(b), the intensity of the white line, observed at 11.562 keV for L_3 and at 13.272 keV for L_2 edges, reduces to a small extent with the decrease in Pt thickness. This reduction for small Pt coverage indicates that the Pt 5d hole number decreases near the interface due to possible charge transfer from Co to Pt atoms.

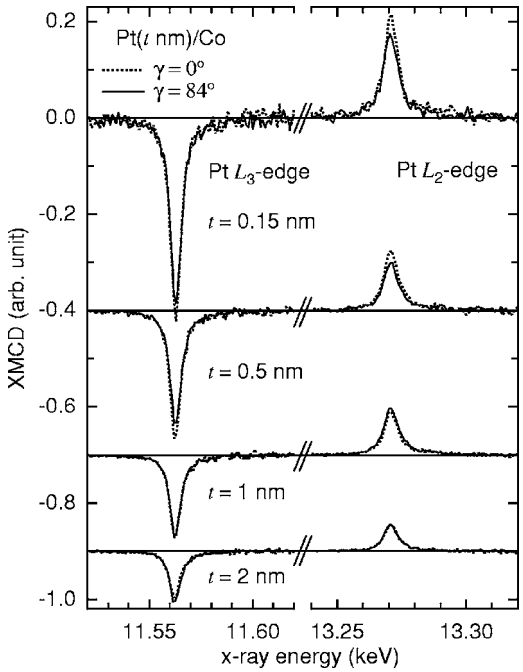

FIG. 4. Comparison of Pt $L_{2,3}$ x-ray magnetic circular dichroism spectra of Pt(t nm)/Co bilayers obtained at $\gamma=0°$ (dot) and $\gamma=84°$ (solid).

In the case of $t=1$- and 2-nm films, all the spectral features are very similar to the bulk Pt. However, the $t=0.15$-nm film exhibits different features, which are primarily characterized by a hump above the white lines at 7 eV. The humps are observed at both the L_3 and L_2 edges and are indicated by arrows in the figure. The feature of the medium coverage—$t=0.5$-nm— film appears to be a mixture of the spectra of 0.15- and 2-nm films. We attribute the hump of $t=0.15$-nm film to the interface Pt atoms. In this film of approximately one monolayer (ML) thickness, almost all Pt atoms are located at the interface with Co and the electronic state may be modified. In the XAS measurement, one can observe a signal averaged over the entire Pt layer; this indicates that the interface contribution would be weak for a sample with a large coverage. We suppose that the 2-nm (9 ML) film consists of one interface monolayer and eight monolayers, in which the electronic states are identical to that of the bulk Pt, on it. In the same manner, the 1-nm (5 ML) film is supposed to be a 1 ML interface and a 4 ML overlayer, and the 0.5-nm (2 ML) film is supposed to be a 1 ML interface and a 1 ML overlayer. In order to verify the hypotheses, we generated an artificial XAS spectrum of a 0.5-nm film from a weighted average of the measured spectra for 0.15- and 2-nm films, considering the interface-to-overlayer ratio assumed above. At the L_3 and L_2 edges, the artificial spectra excellently reproduce the measured ones, as demonstrated in Figs. 3(c) and 3(d).

This analysis has proven that our model is applicable to the present Pt/Co bilayers and that the interface character is identical for all the samples. The electronic state of the interface Pt atom may be modified either by hybridization with the Co atom or by the reduced structural symmetry at the interface. In the second monolayer from the interface and beyond, no drastic change in the electronic state should occur, as far as nonmagnetic electronic states are concerned.

Similar hump structure in XAS spectra are reported in 3 at. % Pt impurities in Fe,[17] and not observed in Co/Pt (Refs. 17,18) and Ni/Pt (Ref. 19) multilayers characterized by relatively thick Pt layers, nor (111) $CoPt_3$ alloy thin films of a well-defined structure.[10] However, some papers reported the hump structure in transition metal-Pt alloys fcc-$Co_{50}Pt_{50}$, bcc-$Fe_{20}Pt_{80}$,[18] and $Co_{75}Pt_{25}$.[20] From these alloy cases, the possible alloying at the Co-Pt interface in our samples is not entirely denied. Nevertheless, our XAS analysis revealed that the nonmagnetic electronic states are altered only in the interface layer and unaltered in the remaining layers on it. We conclude that the alloying, if any, is confined to a single monolayer nearest to the interface.

C. Sum rules

The orbital magnetic moment $m_{\mathrm{orb}}^{\gamma}$ and the spin asymmetry term $[m_{\mathrm{spin}}-7m_T]^{\gamma}$, including the spin magnetic moment m_{spin} and the magnetic dipole moment m_T of the Pt atom, were determined using the sum rules[21,22]

$$-\frac{2}{3}\left[\frac{\Delta A_{L_3}+\Delta A_{L_2}}{A_t}\right]_{\gamma}=\frac{1}{n_h\mu_B}m_{\mathrm{orb}}^{\gamma}, \tag{3}$$

$$-\left[\frac{\Delta A_{L_3}-2\Delta A_{L_2}}{A_t}\right]_{\gamma}=\frac{1}{n_h\mu_B}[m_{\mathrm{spin}}-7m_T]^{\gamma}, \tag{4}$$

where $A_t=\int_{L3}I(E)dE+\int_{L2}I(E)dE$ is the XAS integral summed over the L_3 and L_2 edges; $\Delta A_{L_3}=\int_{L3}\Delta I(E)dE$ and $\Delta A_{L_2}=\int_{L2}\Delta I(E)dE$ are the integrals of the XMCD spectrum at the L_3 and L_2 edges, respectively; n_h denotes the hole number of the Pt 5d band; and μ_B is the Bohr magneton.

In practice, the integrals are determined from the polarization-dependent areas of the near-edge resonances (white lines). For determination of ΔA_{L_3} and ΔA_{L_2}, we approximated an XMCD spectrum at each edge by a Lorentz function and used the areas of the fit function. For determination of A_t, we used the areas of the white line above an edge-jump background (a step function) in the XAS spectrum.[24] The uncertainties in the fitting to separate the white line from the step-like background account for 5% errors in the relative value of resulting magnetic moments. The absolute magnetic moment values, provided in the next subsection, may include systematic errors of $\simeq 10\%$, which arise from both uncertainty in estimation of the hole number and the theoretical error involved in the sum rule analysis.

The XAS integral A_t was used to determine the Pt 5d hole number $n_h(z)$, which may vary with the distance z from the Co-Pt interface. A relation $A_t(t)=C\int_0^t n_h(z)dz/t$ holds between $n_h(z)$ and $A_t(t)$, an integral acquired for a series of samples with different Pt thickness t. Assuming that the outermost Pt of the largest coverage has a hole number of 1.8,[10] we obtain $n_h(z)=1.59$, 1.74, 1.74, 1.8 for $z=0.15$, 0.5, 1.0, 2.0 nm, respectively.

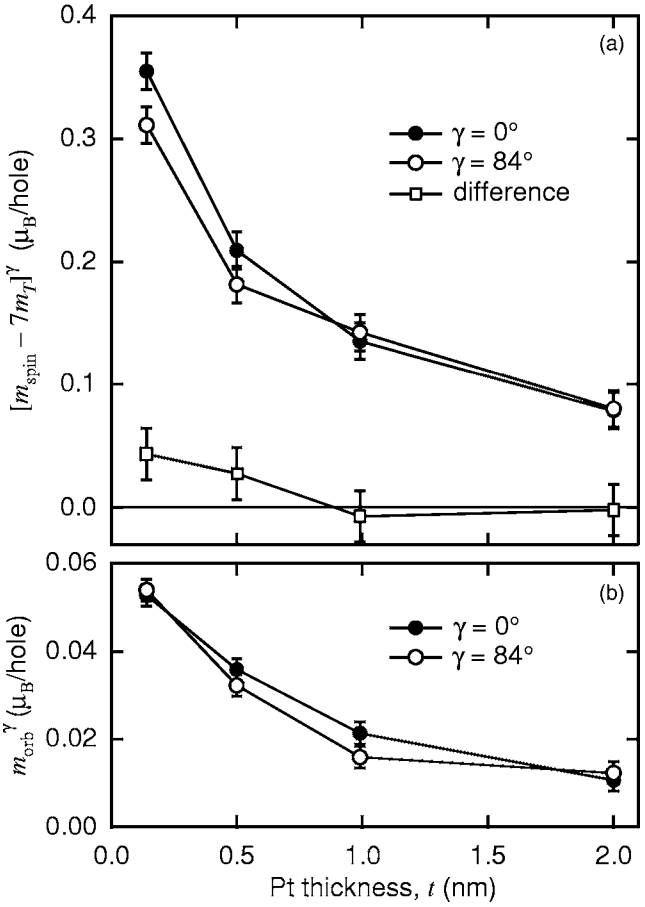

FIG. 5. Pt magnetic moments deduced from the measured dichroism spectra using the sum rules: (a) spin asymmetry terms including spin m_{spin} and magnetic dipole moments m_T, (b) orbital magnetic moments m_{orb}^γ. In both figures, the solid (open) circle denotes the result for $\gamma=0°$ ($\gamma=84°$). The square in (a) shows the difference in the spin asymmetry term for $\gamma=0°$ and 84°.

D. Pt magnetic moments

Figure 5 shows the observed Pt magnetic moments per 5*d* hole as a function of the Pt layer thickness *t*. The spin asymmetry term $[m_{spin}-7m_T]^\gamma$ is shown in Fig. 5(a) and the orbital moment m_{orb}^γ in Fig. 5(b). Larger moments were observed for thinner Pt layers both for $\gamma=0^\circ$ and 84°. This behavior is consistent with the variation of XMCD amplitude with the Pt thickness, which was mentioned in Sec. III A.

The values of $[m_{spin}-7m_T]^\gamma$ show a distinct difference for the $t=0.15$- and 0.5-nm samples, whereas they agree for the $t=1$- and 2-nm samples within the experimental error. For 3*d* transition elements, the variation of MCD spectra with the angle γ is measured in order to determine the anisotropy in the orbital magnetic moment that is closely related to the magnetocrystalline anisotropy and to isolate the spin magnetic moment from the magnetic dipole moment.[25,26] MCD measurements at a "magic angle" ($\gamma=54.7^\circ$) are used to determine the spin magnetic moment value, eliminating the contribution of the magnetic dipole term from the spin sum rule.[26] These angular-dependent MCD measurements in 3*d* systems are based on an assumption that the spin moment of 3*d* electrons is isotropic since the crystal field and spin-orbit coupling are negligible relative to the exchange interaction.[22,27,28] It has been considered that such an assumption is inapplicable to heavy 5*d* elements, such as Pt, because the spin-orbit coupling of 5*d* electrons is typically one order larger than that of 3*d* elements. Nevertheless, the first-principles calculation by Oguchi and Shishidou[28] has recently revealed that the spin moment of 5*d* electrons is isotropic even in a monoatomic Pt layer on Fe (001). This indicates that the angular variation in the spin sum rule arises from the angular-dependent spin dipole term m_T^γ, and thus $[m_{spin}-7m_T]^\gamma$ can be rewritten as $m_{spin}-7m_T^\gamma$ with the constant spin moment m_{spin}, as in the case of a 3*d* system.

TABLE II. Magnetic moments of the Pt atom at the Co-Pt interface.

m_{spin}	m_{orb}	$m_{spin}+m_{orb}$	$7m_T^\parallel$
0.333	0.053	0.386	$0.022\mu_B$/hole
0.529	0.084	0.614	$0.035\mu_B$/atom

In the discussion below, we treat the out-of-plane and in-plane magnetic dipole moment, assuming the absence of in-plane anisotropy in a Pt layer. The value of $m_T^{\gamma=0^\circ}$ is directly used for the out-of-plane moment $m_T^\perp$. For a uniaxial system, we assume that m_T^γ varies as (to lowest order) $m_T^\gamma=m_T^\perp\cos^2\gamma+m_T^\parallel\sin^2\gamma$.[25] Accordingly, we may use the value of $m_T^{\gamma=84^\circ}$ for the in-plane moment $m_T^\parallel$, allowing a difference as small as 1%. After the calculation results for a Fe/Pt system,[28] establishing $m_T^\perp\approx-m_T^\parallel$, the value of m_{spin} is determined by the average $([m_{spin}-7m_T]^{\gamma=0^\circ}+[m_{spin}-7m_T]^{\gamma=84^\circ})/2$, to cancel the $7m_T^\gamma$ term. The magnetic dipole moment should be half of the difference of the two measured values $7m_T^\gamma=\pm([m_{spin}-7m_T]^{\gamma=0^\circ}-[m_{spin}-7m_T]^{\gamma=84^\circ})/2$, where the positive (negative) sign should be assumed for $\gamma=\parallel(\perp)$. The difference corresponding to $7m_T^\parallel-7m_T^\perp$ is shown in Fig. 5(a), and the sign of m_T^γ is consistent with the calculation.[28] m_T^γ should not contribute to magnetic anisotropy since the bare value of m_T^γ (factor seven excluded) is very small, not more than 1% of the spin moment m_{spin}.

The value of the orbital magnetic moments m_{orb}^γ for $\gamma=0^\circ$ and 84° was in good agreement within the experimental error, and no considerable difference was observed in the values for all the Pt thicknesses. In Co-Pt alloy thin films, the angular variation in the Pt orbital moment, which is associated with the perpendicular magnetic anisotropy, has been reported.[10,11] In the Pt/Co bilayer samples used in this study, the Pt orbital moment is shown to be isotropic. This result is inconsistent with the calculations for a Fe/Pt system, which clearly exhibit an angular dependence in the orbital moment of both Fe and Pt.[28] In the text below, we use the angle-averaged orbital moment given by $m_{orb}=(m_{orb}^{\gamma=0^\circ}+2m_{orb}^{\gamma=84^\circ})/3$.[25]

Table II lists the Pt magnetic moments for the $t=0.15$-nm sample. These values correspond to the magnetic moments of a Pt atom that is in all probability located at the interface with Co. The total magnetic moment $m_{spin}+m_{orb}$ is

$0.39\mu_B$/hole, and this value gives $0.61\mu_B$/atom with the use of the Pt 5*d* hole number 1.59 determined in Sec. III C. The magnitude of the Pt magnetic moment obtained in this study is compared to reported values of $Co_{50}Pt_{50}$ alloy thin films ($0.35\mu_B$/atom)[11] and of Ni/Pt multilayers ($0.29\mu_B$/atom).[16] The larger magnetic moment of the present Pt/Co bilayers is probably due to the thick Co ferromagnetic layer. Kerr measurements for a Co wedge grown on Pt(111) revealed that the average magnetization of Co is proportional to the layer thickness.[29] In the present bilayers, the Co layer thickness (15 nm: $\approx$70 ML) is much larger than the magnetic layer (a few ML) in the previously studied multilayers, so that the average magnetization of the Co layer is large and enhances the Pt magnetization. Ferrer *et al.* demonstrated, by resonant magnetic surface x-ray diffraction, that the induced interface Pt magnetic moment increases with the thickness of Co overlayer in Co/Pt(111).[30] A similar trend is also observed in Ni/Pt multilayers with various Ni layer thicknesses reported by Wilhelm *et al.*[16] Consequently, in the present Pt/Co bilayer, a Pt atom at the Co-Pt interface has a magnetic moment comparable to that of bulk Ni ($0.6\mu_B$), which has a similar d^9 electron configuration in an atomic state. The orbital magnetic moment is $0.053\mu_B$/hole ($0.08\mu_B$/atom), which represents a 14% contribution to the total magnetization.

E. Depth profile of Pt magnetization

Figure 5 shows the average magnetic moment per Pt 5*d* hole over the entire layer, which is represented by

$$\bar{m}(t) = \frac{1}{t}\int_0^t \frac{m(z)}{n_h(z)}dz, \tag{5}$$

where $m(z)$ is the distribution function (depth profile) of the magnetic moment inside the Pt layer with a distance z from the Co-Pt interface, and $n_h(z)$ the distribution of the 5*d* hole number. Thus, from the $\bar{m}(t)$ acquired for a series of samples with various Pt thicknesses t, $m(z)$ can be deduced[31] based on the assumption that the magnetization depth profile depends solely on the distance from the interface and not on the thickness of the entire Pt layer. In this analysis, a set of products of the average moment and corresponding Pt thickness $\bar{m}(t)t$ was obtained and then their difference was found. For $n_h(z)$ the values obtained from the white line integral (Sec. III C) were used. Figure 6(a) illustrates the resulting depth profile of the spin magnetic moment $m_{spin}(z)$ and orbital magnetic moment $m_{orb}(z)$ per Pt atom. Both moments are found to decay with increasing distance from the Co-Pt interface. An exponential function

$$m_{tot}(z) = m_0 \exp(-z/\lambda), \tag{6}$$

substantially reproduces the profile of the total moment $m_{tot}(z)=m_{spin}(z)+m_{orb}(z)$ with the decay distance $\lambda = 0.41$ nm. The fit curve is shown by the solid line in Fig. 6(a). The decay distance corresponds to two atomic layers of Pt, characterizing the effective range of magnetic coupling between Co and Pt through the interface. The Pt moment is going to be zero at a distance of more than 1 nm from the interface, and 90% of the total magnetization is concentrated within a 1-nm (four atomic layers) region near the interface.

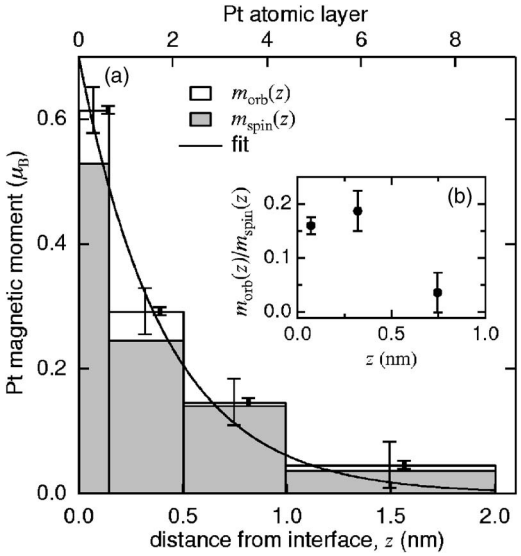

FIG. 6. (a) Distribution of the Pt spin magnetic moment $m_{spin}(z)$ and orbital magnetic moment $m_{orb}(z)$ as a function of the distance z from the Co-Pt interface. Thin vertical lines indicate the experimental error in the total magnetic moment and thick lines indicate the error in the orbital magnetic moment. (b) The ratio of the orbital to the spin magnetic moments $m_{orb}(z)/m_{spin}(z)$ versus z.

The orbital magnetic moment decays more rapidly than the spin moment. In Fig. 6(a), the large orbital magnetic moment is relative to the spin moment in the case of Pt atoms near the interface ($z<0.5$ nm). On the other hand, the ratio appears to be small at a distance from the interface ($z>0.5$ nm) despite the relatively large errors in the moment values in this region. The ratio $m_{orb}(z)/m_{spin}(z)$ is plotted in Fig. 6(b) for $0<z<1$ nm.[32] Near the interface, the ratio $m_{orb}(z)/m_{spin}(z)$ is more than 15% when $z<0.5$ nm, while this ratio drastically decreases when $z>0.5$ nm. The concentration of the orbital moment near the Co-Pt interface may be a source of interfacial magnetic anisotropy, which was recently reported in Co/Pt multilayers by a torque magnetometry measurement.[8] Their study presented the fact that anisotropy energy per unit bilayer increases more rapidly than induced Pt magnetization with an increase in the Pt layer thickness, revealing that the magnetic anisotropy is enhanced at the interface. The region exhibiting the enhanced magnetic anisotropy is 0.3 nm from the Co-Pt interface; it is in good agreement with the region where large orbital moment values are observed in the present study.

The present results provide a guideline for designing a practical magnetic medium of a magnetic-nonmagnetic layered structure although the depth profile might include the effects of local interface roughness or possible alloying limited to one monolayer at the interface, which make the magnetization decay broader as compared with an ideally sharp interface. From the depth profile, only four atomic Pt layers possess nearly the entire magnetization induced through the interface with the magnetic Co layer. These Pt layers could significantly contribute to the improvement in the thermal magnetization stability and thermal demagnetization perfor-

mance in real layered magnetic media. In other words, it is clearly demonstrated that adopting Pt layers thicker than four atomic layers would be ineffective in improving the performance of layered magnetic media. Additionally, the considerable amount of orbital magnetic moment, confined to two atomic layers, may enhance the magnetic anisotropy near the interface; it would contribute to the appearance or enhancement of a perpendicular magnetic anisotropy when the composition and thickness of the magnetic layer is appropriately tailored.

The result obtained indicates that a Pt cap layer, which until now was used to protect the body magnetic layer from corrosion, can improve the thermal magnetization stability. Moreover, the "magnetized" Pt cap layer would ensure tight magnetic coupling between the data recording head and storage medium in data writing/reproducing operations. In other words, it would reduce the "spacing loss" to some extent, although the head and medium are further separated by a few nm (thickness of the corrosion-resistant Pt layer).

The values of the total Pt magnetic moment ($m_0 = 0.61\mu_B$/atom) and the decay distance ($\lambda = 0.41$ nm) obtained in this work are in agreement with the recently reported values in FePt $L1_0$ nanoparticles covered with Pt overlayers ($m_0 = 0.65\mu_B$/atom, $\lambda = 0.44$ nm) by magnetization measurements.[33] Despite the good agreement, it should be noted that the depth profile of Pt magnetization obtained in this study might include small systematic errors because the depth profile may be dependent on the thickness of the entire layer, as predicted by Ederer *et al.*[34] Their theoretical calculations for Co_m-Pt_n multilayer systems, where m and n denote the numbers of the atomic layer in Co and Pt layers, show that in a Co_2-Pt_3 system, the Pt magnetic moment within two atomic layers from the interface is enhanced by $0.05-0.1\ \mu_B$/atom as compared to Co_2-Pt_7 and Co_2-Pt_{13} systems, which have thicker Pt layers. Consequently, corrections for the dependence on the thickness of the entire Pt layer need to be applied for the Pt magnetization depth profile in the Pt/Co bilayer. The correction factor for the present bilayer system should be smaller than that for a multilayer system since in the bilayer, the Pt layer is in contact with the magnetic Co layer only on one side.

The magnetization depth profile obtained in this study is consistent with that determined by resonant x-ray magnetic reflectometry[35] in another Pt/Co bilayer, except for the region within 0.3 nm of the Co-Pt interface, where our results show larger magnetization values. The Pt magnetization profile in that study was determined by fitting the magnetic reflection data to a model profile function that assumes a constant value near the interface within 0.3 nm and decays exponentially in the region beyond this. In the present study, the magnetization profile has been determined independent of any particular model. We have separated the distribution of the spin and orbital magnetic moments and examined the anisotropy of these moments although the orbital moment is found to be isotropic. Moreover, the magnetization in a single atomic Pt layer located very close to the interface has been explored. However, we used four samples with different Pt layer thicknesses to deduce the magnetization profile based on the above-mentioned assumption, assuming that all the properties of the Co magnetic layer and features of the interface would be identical among these samples.

Several XMCD studies have been conducted to investigate the nature of induced magnetization of Pt in multilayers consisting of $3d$ transition metal and Pt layers.[6,7,16] These studies have emphasized the significance of hybridization of wavefunctions of the transition metal and Pt at the interface. Nevertheless, in multilayer systems, the XMCD probes magnetization averaged among multiple interfaces; therefore, an extremely accurate periodicity is required in the layer structure of samples. On the other hand, the samples used in this study were bilayers having a single Co-Pt interface. We have directly observed the Pt magnetization near the interface, which is not periodic. Furthermore, we have obtained clear XMCD signals for an approximately single atomic 0.15-nm-thick Pt layer, and we have determined the quantitative magnetization of the Pt adjacent to the interface with Co.

IV. CONCLUSION

The depth profile of the spin and orbital magnetic moments of a few atomic Pt overlayers of Pt/Co bilayer films have been determined. In the case of the present bilayers, which have a relatively thick magnetic Co layer, a considerably large magnetic moment, $0.61\mu_B$/atom, is induced in the interfacial Pt atoms. The Pt magnetic moment is found to decrease with the distance from the interface as an exponential function, with a characteristic decay length of 0.41 nm. The partial Pt layer within 1 nm (four atomic layers) from the interface possesses 90% of the total magnetization of Pt. The orbital magnetic moment decays more rapidly than the spin moment and the value is more than 15% relative to the spin moment within 0.5 nm from the interface. Anisotropy was not observed in the orbital moment. The magnetic dipole term is estimated to be $0.035\mu_B$/atom, and the anisotropy in the external magnetic field direction exists near the Co-Pt interface.

ACKNOWLEDGMENTS

The authors are indebted to Tamio Oguchi, Tatsuya Shishidou, and Tsuneharu Koide for their fruitful discussions. This work was performed with the approval of the Japan Synchrotron Radiation Research Institute (JASRI) as a Nanotechnology Support Project of The Ministry of Education, Culture, Sports, Science and Technology (Proposal No. 2002B0648-NS2-np, 2003A0463NS2-np/BL39XU).

*Email address: m-suzuki@spring8.or.jp

[1] K. Stoev *et al.* (unpublished).
[2] C. P. Bean and J. D. Livingston, J. Appl. Phys. **30**, 120S (1959).
[3] P.-L. Lu and S. H. Charap, IEEE Trans. Magn. **30**, 4230 (1994).
[4] P. F. Carcia, J. Appl. Phys. **63**, 5066 (1988).
[5] Y. Sonobe *et al.*, IEEE Trans. Magn. **38**, 2006 (2002).
[6] S. Rüegg, G. Schütz, P. Fischer, R. Wienke, W. B. Zeper, and H. Ebert, J. Appl. Phys. **69**, 5655 (1991).
[7] G. Schütz, S. Stähler, M. Knulle, and P. Fischer, J. Appl. Phys. **73**, 6430 (1993).
[8] H. Nemoto and Y. Hosoe, J. Appl. Phys. **97**, 10J109 (2005).
[9] H. Maruyama, F. Matsuoka, K. Kobayashi, and H. Yamazaki, J. Magn. Magn. Mater. **140-144**, 43 (1995).
[10] W. Grange *et al.*, Phys. Rev. B **58**, 6298 (1998).
[11] W. Grange, I. Galanakis, M. Alouani, M. Maret, J. P. Kappler, and A. Rogalev, Phys. Rev. B **62**, 1157 (2000).
[12] Interface alloying becomes significant at ~600 K (Ref. 30). The present films were prepared at a much lower temperature such that the interface mixing should be limited.
[13] D. Weller, G. R. Harp, R. F. C. Farrow, A. Cebollada, and J. Sticht, Phys. Rev. Lett. **72**, 2097 (1994).
[14] H. Maruyama *et al.*, J. Synchrotron Radiat. **6**, 1133 (1999).
[15] P. Lechner *et al.*, Nucl. Instrum. Methods Phys. Res. A **458**, 281 (2001).
[16] F. Wilhelm *et al.*, Phys. Rev. Lett. **85**, 413 (2000).
[17] G. Schütz, R. Wienke, W. Wilhelm, W. Wagner, P. Kienle, R. Zeller, and R. Frahm, Z. Phys. B: Condens. Matter **75**, 495 (1989).
[18] G. Schütz, R. Wienke, W. Wilhelm, W. B. Zeper, H. Ebert, and K. Spörl, J. Appl. Phys. **67**, 4456 (1990).
[19] P. Poulopoulos *et al.*, J. Appl. Phys. **89**, 3874 (2001).
[20] Y. S. Lee, J. Y. Rhee, C. N. Whang, and Y. P. Lee, Phys. Rev. B **68**, 235111 (2003).
[21] B. T. Thole, P. Carra, F. Sette, and G. van der Laan, Phys. Rev. Lett. **68**, 1943 (1992).
[22] P. Carra, B. T. Thole, M. Altarelli, and X. Wang, Phys. Rev. Lett. **70**, 694 (1993).
[23] F. W. Lytle, J. Phys. Chem. **91**, 1251 (1987).
[24] For removing the edge-jump background, we used a minimum fit parameter to determine an arctan step function. The step width was fixed at 3 eV, which is the convolution of the intrinsic line width (Ref. 23) and the monochromator band width; the step height was set to the fluorescence yield measured at much beyond the absorption edge; the threshold energy was only the free parameter. After the edge-jump removal using the determined optimum threshold energy, the XAS white line was found to be a Lorentz function of exactly the same energy center and of equivalent width as the corresponding XMCD spectrum. This similarity holds in the region from 11.530 to 11.569 keV for the L_3 edge and from 13.240 to 13.276 keV for the L_2 edge.
[25] D. Weller, J. Stohr, R. Nakajima, A. Carl, M. G. Samant, C. Chappert, R. Megy, P. Beauvillain, P. Veillet, and G. A. Held, Phys. Rev. Lett. **75**, 3752 (1995).
[26] T. Koide *et al.*, Phys. Rev. Lett. **87**, 257201 (2001).
[27] J. Stohr and H. Konig, Phys. Rev. Lett. **75**, 3748 (1995).
[28] T. Oguchi and T. Shishidou, Phys. Rev. B **70**, 024412 (2004).
[29] N. W. E. McGee, M. T. Johnson, J. J. de Vries, and J. aan de Stegge, J. Appl. Phys. **73**, 3418 (1993).
[30] S. Ferrer, J. Alvarez, E. Lundgren, X. Torrelles, P. Fajardo, and F. Boscherini, Phys. Rev. B **56**, 9848 (1997).
[31] J. Vogel, A. Fontaine, V. Cros, F. Petroff, J.-P. Kappler, G. Krill, A. Rogalev, and J. Goulon, Phys. Rev. B **55**, 3663 (1997).
[32] The data point for $1<z<2$ nm is not shown since the error was abnormally large (~200%) for discussion.
[33] S. Okamoto, O. Kitakami, N. Kikuchi, T. Miyazaki, Y. Shimada, and T.-H. Chiang, J. Phys.: Condens. Matter **16**, 2109 (2004).
[34] C. Ederer, M. Komelj, M. Fahnle, and G. Schutz, Phys. Rev. B **66**, 094413 (2002).
[35] J. Geissler, E. Goering, M. Justen, F. Weigand, G. Schütz, J. Langer, D. Schmitz, H. Maletta, and R. Mattheis, Phys. Rev. B **65**, 020405(R) (2002).